©

Cloud screening over sea-ice and marginal ice zones: Review.

Issue date	*ITT no*	*client*
17/10/2016	15/211424	EUMETSAT

Document Reference
gkt050_010_DL1_1-2

	name	*Date*
Checked by Project Manager		

Editing History

Issue	*Author*	*Date*	*Note*
1.0	G.L.Liberti	20/07/2016	First Version
1.1	G.L.Liberti	15/09/2016	Second Version
1.2	G.L.Liberti	17/10/2016	Minor changes included

TABLE OF CONTENTS

1. Introduction

Within the frame of the EUMETSAT study *'Sea-ice cloud screening for Copernicus Sentinel-3 Sea and Land Surface Temperature Radiometer',* is required as a specific Work Package an '*assessment and summary of current status (in past and on-going projects including published literature) of cloud screening over sea-ice and marginal ice zones for infrared sensors, with a focus on dual-view sensors*' (EUM/OPS-COPER/SOW/15/814091). A review on cloud and sea ice detection over polar regions can be found in Lubin & Massom (2006) and Masson & Lubin (2006) respectively. Even if these texts contain some of the basic concepts used in satellite remote sensing over Polar Regions, they do not take into account the last decade of studies and their review is very general and, therefore, not focused on algorithms and variables that can be applied to the observations from SLSTR. This report summarizes results from studies on cloud detection, in particular over ice/snow surfaces, using data mostly from the (A)ATSR instrument series which is the precursor of SLSTR. In addition, literature using AVHRR-2/3 data is also reviewed being this sensor series the one with the longest available time series of observations. Literature on cloud detection for MODIS, ADEOS-GLI, VIIRS data has also been examined because these instruments have a large number of channels including the new ones on SLSTR (1.3 and 2.2 µm) not available in the (A)ATSR and AVHRR series. Finally, some literature from missions with multiangular observation capability as the POLDER/PARASOL series and MISR have been reviewed even if these sensors are limited to daytime observations. Although quite extensive, literature on cloud detection for VIS-IR imagers on board of geostationary satellite has not been considered as a primary source of information, in this reviewing study, because, due to the orbit characteristics, the information over polar regions is very poor. As a consequence, very few studies, often specific to particular areas, deal with the issue of cloud and sea ice detection (e.g. Temimi et al. 2011). Some results from relevant theoretical and experimental studies on radiative properties of interest for this study have also been included to document the theoretical basis for the concepts used in the sea ice/cloud detection process.

Regarding the cloud detection approach, while this study should focus on Bayesian methods (e.g. Bulgin et. al. 2015, 2014, Pearson et al. 2014, Makie et al. 2010a-b, Merchant et al. 2005, Uddstrom et al. 1999), relevant and applicable concepts can be found in the literature adopting different detection/classification approaches. Large part of the literature describes thresholds-based (both static and dynamic) methods because of their simplicity, low computing resources requirements and practical implementation in operational processing (e.g. Saunders & Kriebel 1988, Massom & Comiso 1994, Ackerman et al. 1998, 2010, Zavody et al. 2000, Ananasso et al. 2003). From an historical point of view cluster analysis or maximum likelihood cloud detection/classification methods (e.g. Eberth 1987, Li 2003, Li 2007) have followed the threshold ones. Afterwards neural network approaches have been developed (e.g. Key et al. 1989, Simpson et al. 2005). Finally, there is a portion of literature using other approaches that can be of interest; it includes fuzzy logic classification (e.g. Baum et al. 1997, Simpson & Keller 1995) and optimal estimation of cloud properties (Poulsen et al. 2012).

The report contains a review (Section 2) on the general concepts used to detect clouds and sea-ice focusing on their applicability to SLSTR observations over polar oceans. Section 3 reviews the variables which have been more frequently used in the detection/classification algorithms as a result of practical implementation of the concepts described in Section 2. A brief review of the validation method used to estimate the skill of cloud detection/classification algorithms is given in Section 4. Section 5, as a summary of this reviewing effort, contains a list of candidate variables that will be used in the successive part of the study to produce the required Probability Density Functions (PDFs).

2. Cloud detection: Physical basis and challenges over polar regions

Cloud detection from satellite observations is, in general, based on the comparison of measured variables against what it is expected to be measured in absence of clouds. In the region of the electromagnetic spectrum covered by the SLSTR (Visible, Near-IR and thermal IR) cloud detection algorithms are based on the following properties of clouds with respect to the surface.

2.1 'Clouds are higher than the surface'

Clouds represent a higher reflecting/emitting surface relative to the land/sea surface. This property, valid for optically thick clouds, is used, in cloud detection algorithms, estimating the pressure (or elevation) of the observed surface and comparing it against the expected value for the surface. Cloud detection algorithms based on this property are similar or are a part of algorithms for cloud top height/pressure (CTH/P) estimation. The theoretical basis behind CTH/P retrieval are the following:

- **Geometrical I**: estimation of cloud top height and cloud detection as a by-product, can be obtained from the detection and analysis of cloud shadow characteristics (e.g CLOUDMAP, 2001). This type of algorithm consists in identifying within the satellite images pixels that are shadowed by a cloud, associating to these pixels the corresponding cloudy ones and using the information on solar illumination and relative position of the cloud and of its shadow to estimate the cloud top elevation. This algorithm can be applied only if solar radiation is illuminating the scene. In addition, over relatively dark surfaces, as for example the open sea, and/or for low illumination conditions the algorithm fails because of the difficulty in detecting cloud shadows. The vertical resolution is limited by the spatial resolution. One of the advantages of such a technique is that is based on geometry, so it does not require calibration of the data. Besides the limitation to the daytime applicability, these algorithms fail to detect extended and vertically homogeneous clouds. Given the above limitations and the relative complexity, for operational processing, in implementing the shadow-cloud matching process this approach is outside the priority targets of interest for this study. However, detection of cloud shadows is of interest to flag pixels before processing them as cloud-free ones (e.g. Hutchinson et al. 2009).
- **Geometrical II**: Satellite derived stereoscopic estimation of cloud top altitude has described quantitatively first by Hasler (1981). Practically, it has been implemented either by using data from the overlapping region of geostationary satellites or by using data from instruments with multiviewing capability such as ATSR (e.g. Lorenz, 1985, Prata & Turner, 1987). Cawkwell et al. (2001) described a cloud detection method using only the 10.8 μm channel, for high latitudes. It is based on the comparison of target altitude, estimated by a stereoscopic method, against radar altimeter derived DEM. The algorithm is applied to the detection of clouds in SE Greenland. Similarly, Muller et al. (2007) developed an algorithm that improved the matching procedure, through the application of sophisticated image processing techniques, and applied their algorithm to ATSR observations over Greenland (Fisher & Muller, 2012).

- **Absorption/Emission based:** Cloud detection, particularly over land, is difficult because of the variability of the contribution from the surface. In the visible, in addition to the temporal and spatial variability of surface radiative properties of a specific surface type, bidirectional reflectance characteristics introduce an additional source of variability. In the thermal IR variability of emissivity and of skin surface temperature can be responsible for spatial and temporal variability of surface contribution to the measured radiances. Absorption by atmospheric gases can be used to decrease or even mask the surface contribution. As a consequence, this kind of approach fails to detect low clouds but it can be very efficient in detecting optically thin cirrus as in the case of the techniques based on the WV absorption band at 1.38 μm (Gao et al. 1993, 1998). Besides the 1.38 μm WV absorption channel other absorption regions have been employed:
- the O_2 A-band (e.g. Buriez et al. 1997);
- the 13-14 μm CO_2 band with different techniques as, for example: CO_2 slicing (Menzel et al. 1983), MLEV (Huang et al. 2004), single TB test (Ackerman et al. 1998, 2010);
- the 0.94 μm (Wind et al. 2010) and 6-7 μm (Ackerman et al. 1998, 2010) WV absorption bands.

Concerning SLSTR, the only channel in an absorption band is the 1.38 μm one (available only in presence of solar radiation), therefore other absorption/emission based methods cannot be applied. However, cloud tests based on thermal IR multi-angular observations (e.g. Zavody et al. 2000) are based on atmospheric absorption properties even if using relatively transparent channels. Relatively weak absorption, particularly from WV, is responsible for differences among window channels. Multiangular tests estimate the expected difference, in the forward viewing geometry, from the one observed for the corresponding nadir viewing geometry and compare it against the observed one. The estimate, is based on statistical relationships obtained for cloud-free scenes, and it will differ from the observed difference is case of presence of clouds, because of the masking of atmospheric layers below a cloud.

- **Molecular scattering based**. A set of cloud detection algorithms is based on the analysis of the effects of molecular scattering on the measured signal. Molecular scattering is a relatively well characterized physical process (e.g. Eberhard, 2010). Uncertainty on the estimated contribution from molecular scattering due to the variability of surface atmospheric pressure is within a reduced range with respect to the one of the cloud top pressure. Variability for atmospheric composition is responsible for an even lower level of uncertainty. On this basis, knowing the elevation of the observed scene (and using ancillary data to estimate the actual surface pressure value) it is possible to estimate the contribution due to molecular scattering , in the measured radiance. In the UV-VIS spectral regions, where the molecular scattering is used as 'known signal' optically thick clouds mask the molecular contribution from the layers below the cloud top. Therefore, by comparing the measured values with that expected for cloud free atmosphere it is possible to detect the presence of a cloud. Based on a similar assumption as the multiangular detection method based on absorption discussed above (e.g. Zavody et al. 2000), Di Girolamo & Davies (1994) suggest, for the MISR mission, a method to detect cirrus clouds based on the multiangular/multispectral analysis of signal using, as a reference, what expected from molecular scattering. Besides the fact that similar algorithms are limited to daytime, their practical implementation, except for few cases (Di Girolamo & Davies 1994), is are mostly funded on the analysis of the polarization of the measured signal (e.g. Buriez et al. 1997) or even on the effects of Rotational Raman scattering (Vasilkov et al. 2008). The reviewed literature cloud detection based on the analysis of molecular scattering component employs multiangular-multispectral observations and/or measurements of polarization components or high spectral resolution/low noise radiances, as needed for estimation of Ring effect. This type of measurements allows to identify the molecular scattering contribution from the total measured signal. However, instruments able to give the measurements with these characteristics are demanding in terms of instrument design compared to the majority of VIS-IR radiometer. On the basis of the above considerations, cloud detection method based on the analysis of contribution of molecular scattering does not seems to be a promising approach to be applied to the detection of clouds over polar oceans from SLSTR.

2.2 'Clouds are colder than the surface'

Cloud detection based on the hypothesis that clouds are colder than the surface combines the properties that clouds are elevated, with respect to the surface, with the assumption of decreasing temperature with the altitude. Practically the detection based on this concept is generally implemented by comparing the brightness temperature of a relatively transparent channel (the most frequent choice is a channel in the 10-12 μm window) against a threshold value. An example, of a test based on this concept is the '*gross cloud test*' in Zavody et al. (2000). About the channel to be used, the most common options are the 11 μm and the 12 μm. Measurements around 11 μm offer the advantage of being less sensitive to water vapor absorption while measurements at 12 μm are more affected by water vapor absorption but also more sensitive to occurrence of thin clouds particularly if formed by ice. This sensitivity derives from the spectral dependence of the imaginary part of the ice (Warren & Brandt 2008). The threshold is generally function of time and space (see discussion in Section 3). Besides the issue to adapt the discrimination threshold/PDF's or similar to the cloud free environmental conditions, these methods typically fail for effective optically thin clouds (i.e. optically thin cloud filling the pixel FOV or optically thick cloud partially filling the pixel FOV), particularly over warm surface because the measured brightness temperature can be in the range of expected variability of the cloud free one, particularly over land surfaces. Over polar regions, due the frequent occurrence of atmospheric inversions, particularly during the polar night and over land, cloud detection methods based on the hypothesis that clouds are colder than the surface are likely to fail. On the other hand, the frequent occurrence of anomalous vertical structure of the atmosphere has been used to define a different set of variables also based on thermal IR channels. A variable sensible to the presence of clouds for regimes characterized by frequent occurrence of strong inversions at the surface, is given by the difference between a brightness temperature in the atmospheric window at 10-12 μm and one in the WV absorption region 6-7 μm (Liu et al. 2004). In absence of clouds the window channel is colder than the WV one whose signal contains the contribution from the emission by WV molecules (at a temperature warmer than the surface) above the inversion layer. In presence of clouds, which typically forms above the inversion level, both channels measure similar temperatures.

2.3 'Clouds are a bright surface'

In the visible, optically thick clouds are characterized by a reflectance larger than that of most of the natural surfaces. This is due to the very low absorption by condensed water and by the dimension of the cloud scattering particles. Tests based on this property classify as cloudy observations with reflectance larger than the expected value for the surface in absence of clouds. They are generally based on the analysis of reflectance measured in a single channel (typical of first generation geostationary radiometers). In addition to the daytime limitation, this test is efficient for relatively dark surfaces, as for example for the ocean in the SWIR range but it can fail over bright surfaces such as, deserts, snow or vegetation in the 0.8 μm region. For bright surfaces the analysis of the *color* of the observed scene (see next Subsection), using at least two measurements is employed to discriminate between bright surfaces other than clouds and clouds. Over oceans, single reflectance based cloud detection fails, in general, in the detection of very optically thin clouds due to their low reflectance value. Another case of expected failure if represented by measurements in *sun-glint* conditions: i.e. specular reflection of direct solar radiation occurring for a particular geometry. Sun-glint reflectance characteristics have been described by several authors starting from Cox & Munk (1954a-b), not only because of the ambiguity (large spectrally neutral reflectance) with the cloud signal but also because sun-glint, as the cloud contamination, is an important limiting factor for ocean color missions. For multiviewing missions such as SLSTR, the ambiguity cloud-sunglint can be easily solved by comparing the two viewing geometries because the sunglint conditions can occur only for one of the two geometries. Finally, sunglint, providing an estimate on surface wind characteristics, can be used as a known signal, as the molecular scattering, for several applications including vicarious calibration (e.g. Sayer et al. 2010, Zavody et al. 1998).

2.4 'Clouds are white'

Clouds are spectrally neutral in the visible. This is due to the combination of two factors occurring over clouds: the relatively low value of the imaginary part of the water/ice refractive index in the visible and the relatively large size parameter of cloud particles in the visible range. Cloud detection tests based on this concept generally compare reflectance in different part of the spectral region 0.4-1.0 μm testing the hypothesis that clouds reflectance should be the same in that interval. Example of cloud detection tests based on this assumption are NDVI based ones, as well as tests based on the difference or ratio of the channels at 0.6 and 0.8 μm (e.g. Saunders & Kriebel 1988). Over ice/snow surfaces, while in the visible, snow is still relatively 'white', in the SWIR because of the combination of relatively larger imaginary part of the ice complex refractive index and larger dimensions, with respect to cloud ice particles, of the scattering ice volumes, effects of absorption are evident (see fig.1) in the reflectance spectrum. This allows, combining measurements in the visible and in the SWIR to be able to separate clouds from snow/ice.

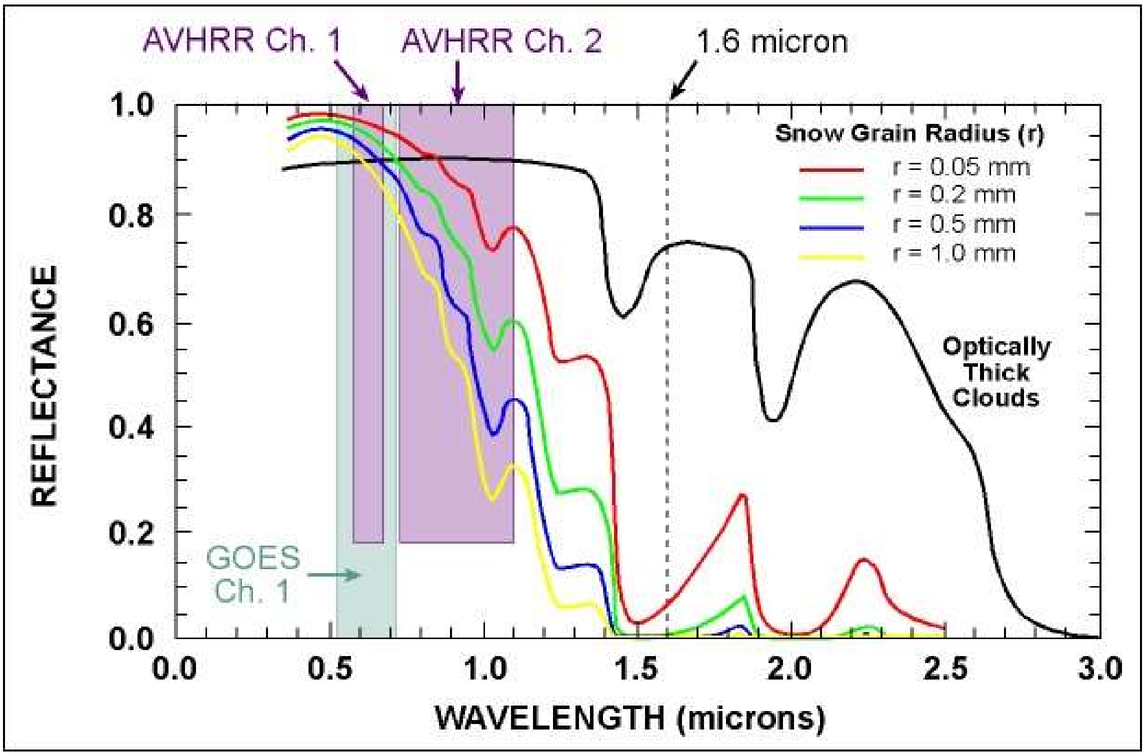

Figure 1. Satellite channel wavelengths in microns (μm), and typical reflectance spectra for snow and cloud (from http://www.nohrsc.noaa.gov/technology/avhrr3a/avhrr3a.html)

2.5 'Clouds have high spatial variability'

Detection of clouds based on the analysis of spatial variability over a limited area is based on the hypothesis that the cloud-free surfaces are relatively homogeneous (e.g. Key & Barry (1989), Martins et al. (2002)). This is generally true over oceans for both VIS, NIR and TIR observations. Over land surfaces, this is a weaker assumption due to the effect on radiative properties (reflectance and/or emissivity) of the variability of surface properties: e.g. land cover, land surface temperature, soil moisture. Even over oceans, spatial variability cloud detection tests are likely to fail in regions of strong thermal and/or optical (e.g. chlorophyll, suspended sediment) gradients where the most interesting processes, from the point of view of physical oceanography as well as for marine fisheries applications, generally occur. Typical examples of incorrectly classified cloudy pixel occur, for instance over the front of the Gulf Stream Current. Similar cloud detection schemes can be implemented using different way to estimate the spatial variability: histograms, local variance and more complex textural variables. In addition to algorithms that estimate the variability of the signal for a set of pixels, the cloud spatial variability is also used to detect partially filled cloud pixels. This is generally done comparing brightness temperatures in the two atmospheric windows at 3-4 μm and 10-12 μm. Pixels which contain in the FOV not homogeneous surfaces, as partially cloud covered ones, due to the different radiance-temperature dependence in the two window regions, show larger brightness temperature differences, compared to pixels sensing homogeneous scenes.

2.6 'Clouds have high temporal variability'

Cloud detection algorithm can be based on the hypothesis that clouds properties have a higher temporal variability than surface ones. Clouds are detected from the analysis of time-sequences of data, assuming that any short-term change in observed radiances can only be introduced by clouds (e.g. Key and Barry, 1989; Diner et al., 1999; Lyapustin et al., 2008; Lyapustin & Wang, 2009; Gafurov and Bardossy, 2009).

2.7 'Clouds are composed of particles of condensed water'

Cloud detection tests based on the concept that a cloud is composed by particles of condensed (liquid/solid) water, generally utilize spectral combination of observations that are able to identify typical radiative (scattering and/or absorption/emission) signature of condensed (liquid/solid) water. Instruments with possibility of multiangular analysis (e.g. POLDER, PARASOL) also identify, in the measured radiances, angular signatures that are typical of some kind of clouds as for example the rainbow scattering maxima around 140° of scattering angle typical of water droplets. (NB: Cloud tests based on the spectrally neutral behavior of clouds in the visible range ('*clouds are white'*) are actually a subset of test based on the concept that clouds are composed of particles of condensed water)

The optical properties depend from size and shape (habit) of the condensed water particles as well as, from the spectral behavior of both components of the complex refractive index (e.g. Warren & Brandt 2008, Kuo et al. 1993, Hale & Querry 1973). In particular, most of the spectral variables used for cloud detection/classification are derived from the spectral dependence of the complex part of the refractive index (Fig.2). Over the Polar regions (as well as over snow covered surfaces) cloud detection based on this concept may fail because the surface is also composed of condensed water. The main difference, that is used to distinguish between surface and cloud in these cases, is in the dimension of the ice particles. The surface is generally characterized by larger size, slab surfaces for thick aged ice.

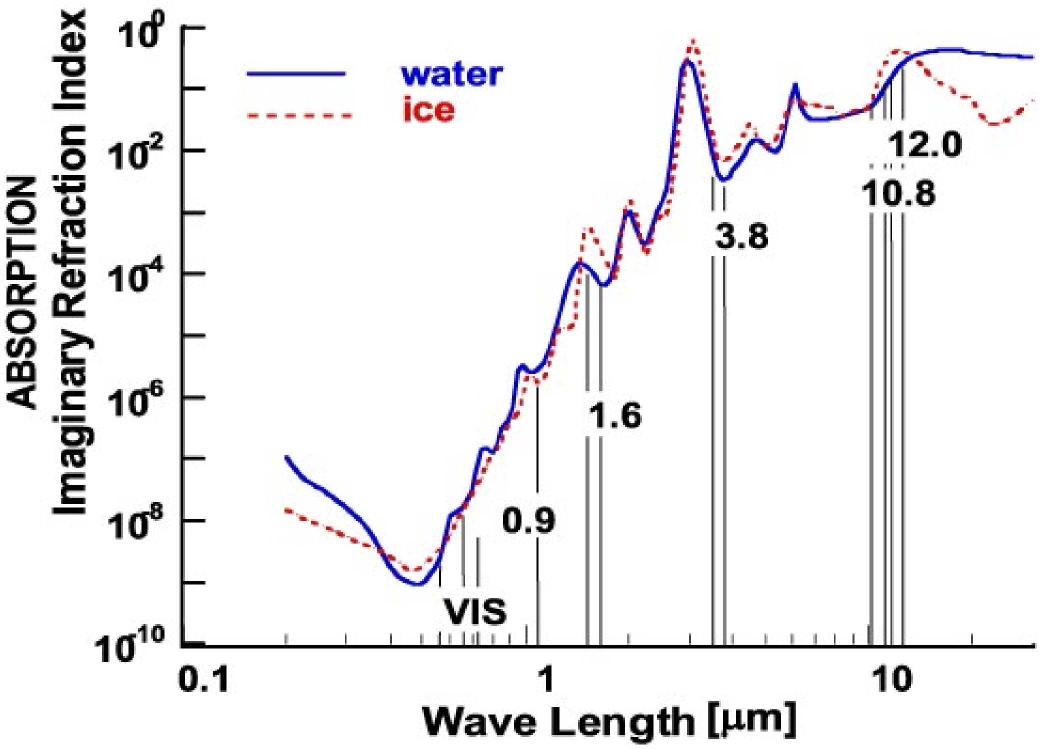

Figure.2. Spectral dependence in the complex part of the refractive index for liquid and solid water

2.8 Sea-Ice Cloud discrimination

A requirement of this study is the discrimination between Sea-Ice and Clouds. In addition to the literature dealing exactly with the sea-ice detection, we can get useful information also from the literature about snow detection and snow properties estimation, due to the probability that sea ice can be covered by snow. Discriminating clouds from sea-ice and snow is particularly difficult because of the similarities between the two scenes. The physical basis used in literature to distinguish between the two surface types from VIS-IR imagery are the following:

- **Temporal variability:** clouds are assumed to have a higher temporal variability than sea-ice (and snow);
- **Spatial characteristics:** due to the lack of spectral and temporal information in the first generation of VIS-IR imager (e.g. the AVHRR-2 series) a particular effort has been done to explore the information content in textural variables (e.g. Eberth 1987, 1989, 1982). The rationale for a classification based on textural variables is that the two surface types are expected to have a different spatial organization due to the different processes and environments generating the two surface types.
- **Geometry of the scattering/emitting condensed water**. While textural variables classification skills are due to the difference between clouds and sea-ice in terms of macrophysical characteristics and therefore require the estimation of textural variables over a set of pixels, the different microphysical characteristics (dimension, geometry and orientation) of the condensed water in the two surface types generate different scattering/emitting properties that can be observed, with multispectral and/or multiangular observation in a single pixel (e.g Hori et al. 2006).

2.9 Summary

Focusing on the objective of this study, that is to produce PDF's for an operational classification of over SLSTR observations over polar oceans in three classes (ocean, sea-ice, cloud), it is evident that the task is particularly challenging. Concerning the reviewed concepts at the basis of cloud detection the particular geographical region and the instrument characteristics limit the applicability of a portion of the concepts used.

Firstly, even if the solar channels contain useful information for cloud detection, the absence of solar radiation for part of the year, suggests to base the sea-ice cloud detection on methods that can be applied to thermal channels.

The absence of absorbing channels (with the exception of the 1.3 μm) limits the applicability of cloud methods based on the difference between the observed signal and the one expected for clear sky in absorbing bands. In addition, any technique based on cloud top estimation/comparison should take into account that in Polar regions clouds are relatively close to the surface and their geometrical thickness is relatively low.

Operational constraints also limit the applicability of cloud detection techniques based on complex analysis of spatial and temporal variability.

3. Cloud detection variables

This section contains a review of the most frequent variables adopted for cloud detection, that can also be obtained from the set of measurements available from SLSTR. The information content in the reviewed variables, in terms of cloud/sea-ice detection, derives from the sensitivity of each variable to the cloud detection concepts identified in the previous section.

3.1 Spectral variables

Single channel brightness temperature: Single channel brightness temperatures are used as discriminating variables on the basis of the principle that clouds are colder than the surface. This kind of relatively simple test is generally called '*gross test*'. The most frequently used channel is the 10-11 μm window channel (**BT11**).

For example, over ocean MODIS cloud detection (Ackerman et al. 1998, 2010) adopt a set of fixed global thresholds for **BT11**: 267, 270, and 273 K for low, middle, and high confidence of clear sky, respectively. Relatively warm (low stratus) and/or relatively optically thin clouds (thin cirrus, partially covering clouds) fail to be detected from a similar set of thresholds, particularly over warm oceans. Over polar oceans, clear ocean pixels may have **BT11**<273 K due to the fact that ocean water freezes at about 271 K and additional atmospheric absorption, even if it is weak for typical polar atmospheres, causes an additional reduction of the radiance emerging from the top of atmosphere. As an example, on the basis of the above considerations Zavody et al. (2000) set the minimum allowed **BT11** value for clear sky scene to 268.7 and 266.8 K for nadir and forward view respectively. For polar regions, besides the need for specific threshold values (not strictly needed if a Bayesian approach is adopted) the overall concept of clouds colder than the surface cannot be applied because of the frequent occurrence of atmospheric inversions (see Sect.2).

Birks (2007) uses for the *'gross cloud test'* the less transparent 12 μm channel (**BT12**) because clouds tend to have a greater optical depth at this wavelength than in the shorter wavelength channels (Saunders & Kriebel, 1988). The thresholds for this test are provided in a look-up table (LUT) of climatological mean surface temperature as a function of latitude and month. These LUTs were constructed from ground station measurements made between 1961 and 1990, interpolated onto one-degree latitude bands (New et al. 2002).

Alternatively, to the use of the 10-12 μm window channel other single channels Tb's are used to detect clouds, particularly high clouds. This is the case of tests based on brightness temperatures in absorption (WV **BT6.7** or CO_2 **BT13.9**) channels (Ackerman et al. 1998, 2010). The rationale for using such absorbing channels is the fact that the surface (and low clouds) contribution is absorbed and therefore even for relatively warm surfaces the problem of the background and its variability is reduced.

According to Simpson el al (2005) over ocean and for daytime observations single brightness temperature (e.g. **BT11**) is not a key variable for their neural network cloud detection method. However, besides the fact that they discuss only the case of cloud detection over ocean and in daytime, conditions favorable for solar channel based algorithms, they still use the **BT11** as post processing variable to discriminate between sun-glint and cloudy pixels.

Single channel brightness temperature – climatology/forecast: *Gross cloud tests* (i.e. tests based on the comparison of measured Tb against a fixed globally valid threshold (or a set of confidence dependent thresholds) are very simple and therefore computationally efficient, however they may fail in regions with extreme climate such as polar regions. In order to account for the local meteorological conditions single channel threshold values can be expressed as a function of a variable like the SST. As an example, Figure 3 (upper panels) show the PDF's of **BT11**, **BT11-BT12** channel combination for two extreme SST classes (272.5-275.0 K and 300.0-302.5 K) as reported in Pearson et al. (2014). However, introducing, SST (or similar variable) dependent thresholds/PDF's increase the skill of the cloud detection process but increase the complexity and can introduce artefact when passing from one SST class to a different one. On the basis of the assumption that air temperature and water vapor are, as an average, strongly related to SST and that, as consequence, also the water vapor condensation will be modulated by the SST, it is possible to use, for cloud detection, rather than the **BT11** value the difference **BT11-SST**. Figure 3 (middle and lower panels) show the PDF's of **BT11-SST**, **BT11-BT12** variables combination for two SST classes (282.5 K and 292.5) for nadir and forward view. The PDFs in the lower and middle panels are relatively similar. Their reference SST differ only for 10 K, compared to the upper panels that refer to two extreme SST classes, but for a given climate region as the polar oceans the annual range of variability should be close to 10 K.

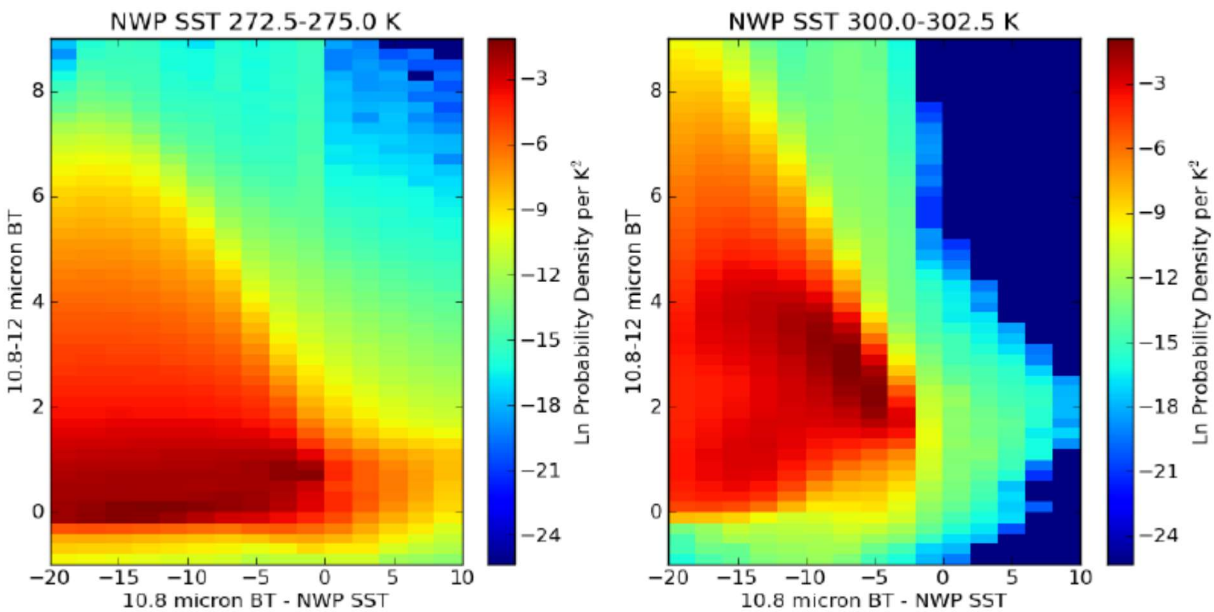

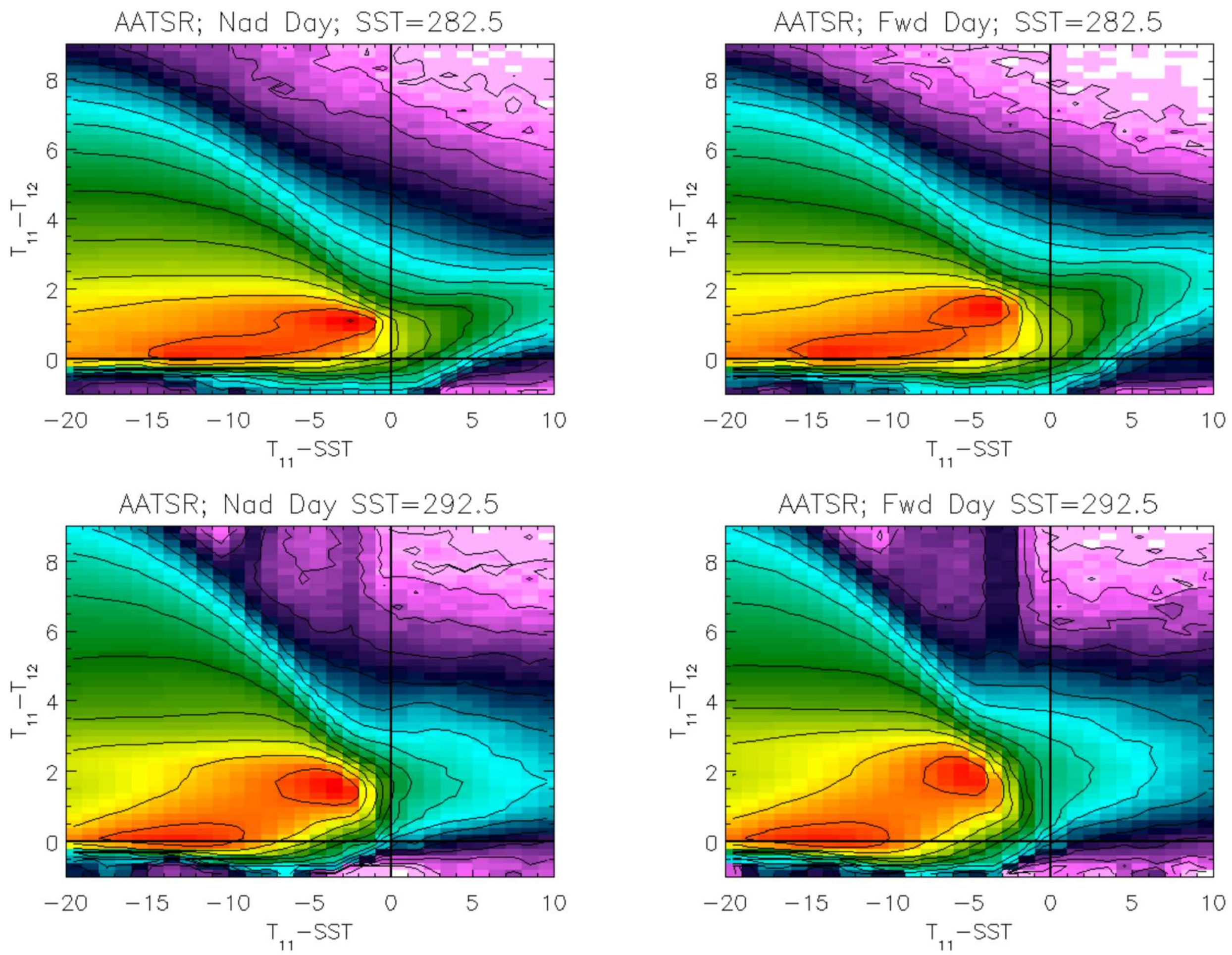

Figure 3. Upper panel. Examples thermal spectral PDFs for **BT11** vs **BT11-BT12** for two NWP SST values. Middle and lower panel. Examples thermal spectral PDFs for **BT11-SST** vs **BT11-BT12** for two NWP SST values and for forward and nadir view (from Pearson et al. 2004).

BT11-BT12. The split window brightness temperatures difference is used to detect cirrus clouds over oceans. Over oceans, this difference, in absence of clouds is mostly proportional to the absorption/emission from atmospheric water vapor. The strength of this spectral variable to detect clouds, in particular thin cirrus (Inoue, 1985), derives from the relatively large difference in the complex part of ice refractive index between 10 and 12 µm (larger at 12 µm). In presence of optically thin cirrus this difference can be larger than what expected from atmospheric water vapour. Over mid/low latitude oceans this test is very efficient, once tuned for the expected WV amount, to detect thin cirrus that would pass the simple brightness temperature test. In absence of solar radiation, this test is one of the most consolidated cirrus detection test. Over polar oceans, the presence of atmospheric inversions and of sea ice, reduces the skill of this test (Yamanouchi et al. 1987).

BT11-BT3.7 The analysis of the difference between brightness temperatures in the two atmospheric windows 3-4 µm and 10-12 µm contains useful information for cloud detection purposes through the combination of different physical processes:

- Detection of partially filled cloud pixels is possible by analyzing this brightness temperature difference due to the large difference in the relationship relating radiance to brightness temperature (Planck law) for typical observed scenes.

- During daytime the cloud reflectance properties in the 3-4 μm window allow identification of features particularly over convective systems. Also over ice this channel combination contains information to identify different surface types (e.g. Yamanouchi et al. 1987).
- At nighttime this test is particularly useful to detect fog and low stratus that being relatively warm are difficult to detect with 'gross cloud tests'. The physical basis for this test derive mostly from the difference in the imaginary part of the refractive index in the two atmospheric windows (see fig.2), partly to the different scattering properties due to a combination of different real part of the complex refractive index and size parameter. Due to this difference, for example, stratus and fog have higher emissivity at 11 μm (about 0.99) than at 3.7 μm (0.8–0.9), and hence it increases **BT11-BT3.7** difference. Similarly, for ice clouds the absorption/emission in the 10-12 μm window is larger than in the 3-4 μm.

Liu et al. (2004) for detection of clouds over polar region at nighttime, suggest the use of the **BT12** instead of the **BT1**1 in the difference because of the larger difference between the imaginary part of the refractive indices of both ice and water. While **BT11** is generally adopted to avoid false alarm due to water vapour absorption, due to the low amount of water vapour in polar atmosphere, particularly during polar winter, the larger sensitivity of the **BT12-BT3.7** difference to clouds can be used with lower probability of false alarm detection due to water vapour absorption.

Finally, in literature other brightness temperature combination including channels in atmospheric IR window region not available in SLSTR are found. For example, MODIS cloud detection (Ackerman et al. 1998) include also tests on the difference **BT8.7-BT11**, while, over polar regions, for VIIRS, a useful information to discriminate during daytime between water clouds and sea-ice is documented for the difference **BT3.7-BT4.0** (Hutchinson et al. 2013a, 2013b).

Single channel reflectance: Single channels reflectance are used to discriminate clouds on the basis that clouds are bright surfaces. Besides what already discussed on the validity of this assumptions, single channel reflectance cloud detection mostly uses measurements in the 0.8 μm (**R0.8**) spectral region. This is due to the fact that, compared with the other historically available channel in the 0.6 μm (**R0.6**) spectral region, sea surface is relatively dark, while sediments may be responsible for a variable contribution from the sea surface to the TOA signal, and also atmospheric scattering, in particular molecular one, is reduced. The availability on the AVHRR-3, started in 1998 (NOAA-15), of a channel in the atmospheric window at 1.6 μm (**R1.6**), introduced the use of the reflectance measured in this channel as a valuable variable to detect clouds. In addition to the information carried by this channel on cloud top phase, reflectance at 1.6 μm is characterized by even lower cloud free (aerosols and molecular scattering) and sea surface contribution. In some cloud detection algorithms (e.g. Zavody et al. 2000, Pearson et al. 2014) **R1.6** is the only information used as single reflectance.

R2.2. Compared to (A)ATSR and AVHRR-2/3 series SLSTR will carry an additional channel measuring reflected solar radiation at 2.2 μm (**R2.2**). MODIS standard cloud detection (Ackerman et al. 1998, 2010) does not use this channel. Pearson et al. (2014), on this basis and observing that, over oceans, **R1.6** and **R2.2** show similar characteristics, do not assign as a priority the use of this channel for cloud detection. On the other hand, However Li et al. (2007) as a result of their study suggest that 2.13 μm band could be used for detection of low level thin clouds.

Average Albedo: Simpson et al. (2005) utilizes, in their neural network approach, an average albedo defined as the average of all valid visible channel albedos (up to 3). They use the average rather than a single channel one because of the highly variable quality of single visible channels of the ATSR-2. From the point of view of cloud detection, because the channels used are the visible ones, their albedo value should be practically the same in case of cloud.

R.1.3: The first portion in the solar spectrum where for most of the cases atmosphere is completely opaque is the WV absorption band at about 1.3 μm. Only in presence of high cloud reflected radiation can emerge from the atmosphere. The absence of contribution from the surface allows for the detection of thin cirrus clouds even over bright surfaces including low level clouds (Gao et al. 1993) and polar regions (Gao et al. 1998). A channel in the 1.3 μm WV absorption band was first carried by the MODIS instruments and because of its efficiency it is now included in a large set of instruments in current and future satellite missions.

Normalized Difference Vegetation Index (NDVI): defined as:

$$\mathbf{NDVI = (R0.8 - R0.6)/(R0.8 + R0.6)}$$

was originally developed to distinguish, over land, clouds from relatively bright (at 0.8 μm) vegetated surfaces (Tucker 1979). The principles on which cloud detection is based in that '*clouds are white*' while vegetation, that can be even brighter than optically thin clouds at 0.8 μm has a strong spectral dependence being an efficient absorber in the red portion of the visible spectrum (0.6 μm).

Over ice/snow different sensitivity to the snow grain size, due to the different size parameter of the scattering condensed ice, is already occurring for this 'historical' spectral regions. **R0.6** is affected only by a few percent variability of reflectance due to the variability of snow grain size while for **R0.8** may be as large as 20% (Domine et al. (2008), Wiscombe & Warren (1980), Tedesco & Kokhanovsky (2007)). This different sensitivity justifies the observed skill of combination of these two reflectances in discriminating clouds from ice/snow.

Similar information than the one obtained from the NDVI can be obtained from other combinations of the **R0.6** and **R0.8** channels. Variables defined as (**R0.8-R0.6), (R0.8-R0.6)/R0.8** or **R0.8/R0.6** are also found in literature.

Normalized Difference Snow Index (NDSI) is defined (Salomonson & Appel 2004) in a similar way than the NDVI as:

$$\mathbf{NDSI = (R0.55 - R1.6)/(R0.55 + R1.6)}$$

The skill of this index is due to the different absorption properties of ice that is not absorbing at 0.55 μm while is absorbing at 1.6 μm (liquid water is also absorbing at this wavelength but in a weaker way compared to ice). From the occurrence of absorption within the scattering ice particles derives also a sensitivity to their dimension. The usefulness of the NDSI is based on the fact that snow and ice are considerably more reflective in the visible than in the shortwave IR part of the spectrum, and the reflectance of most clouds remains high in the short-wave IR, while the reflectance of snow is low being formed by larger ice particles.

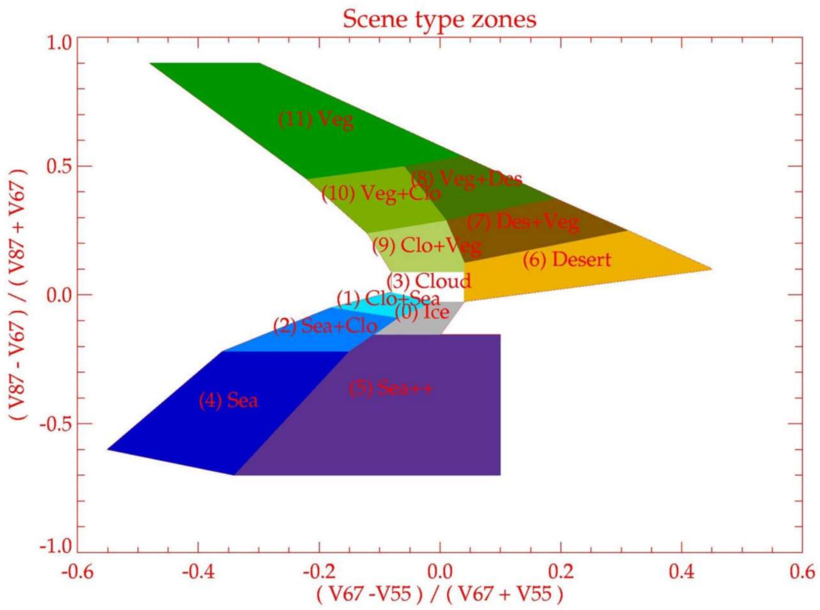

Figure 4. Example of surface type zones classification for the combination **NDVI** and **NDI2** (Birks 2007)

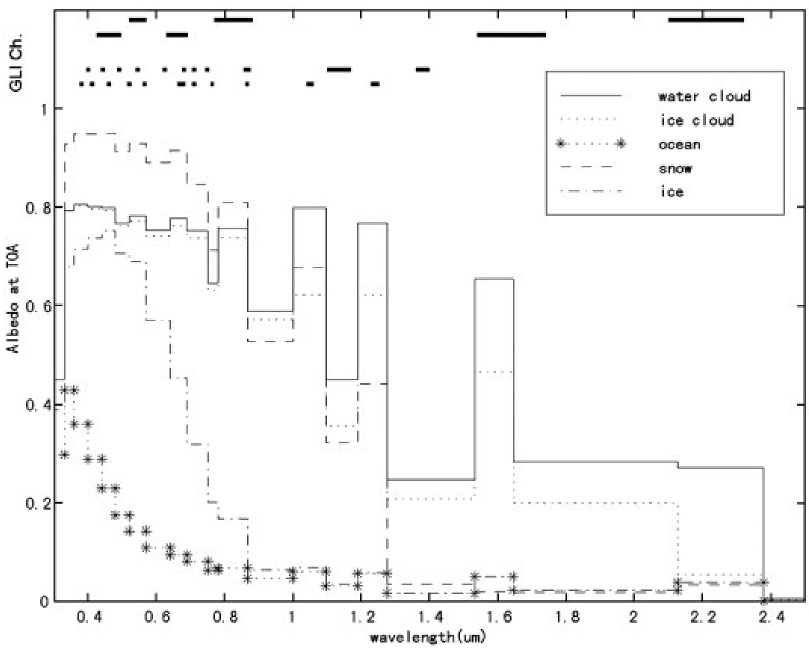

Figure 5. Planetary albedo-values of various types of surfaces and clouds in the spectral range between 0.3 and 2.5 μm for solar zenith angle θ=60°. The location and bandwidth of GLI channels 1–29 are also shown at the top part of the figure with black dots or lines. (Stamnes et al. 2007)

Other Normalized Difference Solar Reflectance Based Indices: Other combinations of channels in form of normalized difference indices can be defined with the solar channels available on SLSTR. Birks (2007) investigates two indices defined as:

NDI2 = (R0.6 – R0.55)/(R0.67 + R0.55)

and

NDI3 = (R0.87 – R0.55)/(R0.87 + R0.55)

as a result, they found some classification skill when combining **NDVI** and **NDI2** (see fig.4).

Stamnes et al (2007) define for the GLI data a **Normalized Difference Ice Index** (**NDII**) as:

$$\mathbf{NDII = (R0.545 - R1.05)/(R0.545 + R1.05)}$$

to distinguish between snow and sea-ice. In the Visible sea ice has characteristics relatively similar to snow, while in the spectral region 0.6–1.2 μm there is a difference in albedo between snow and sea-ice (see fig.5). Due to the strong absorption of sea-ice, the planetary albedo of sea-ice drops rapidly at 0.6 μm, while snow maintains a relatively high albedo until 1.2 μm. On the other hand, a channel centered at 1.05 μm, wavelength also used by Nolin & Dozier (1993) for the estimation with AVIRIS of snow grain size, is not common on satellite radiometers

3.2 Textural variables

Textural variables are based on the hypothesis that sea surface is a more spatially homogeneous than cloud (sea-ice). The more frequently adopted textural variable is the local standard deviation LSD (or variance) over a 3x3 pixel box.

The lack of contrast of clouds over surface in polar regions, particularly during the polar night, and the relatively poor spectral information in the first generation of VIS-IR imagers generated an interest in the analysis of textural features derived from generic image classification studies (e.g. Haralick et al. 1973). Several authors introduced textural variables in the cloud detection scheme over polar regions (e.g. Ebert, 1987, 1989, 1992, Key 1990, Welch et al. 1990, 1992, Penaloza & Welch 1996, Coakley & Bretherton, 1982). One issue when using textural variables is the size of the box used to estimate the texture variables. Complex textural variables may need relatively large boxes and therefore give a cloud detection product at a reduced spatial resolution compared to the original observations.

Simpson et al. (2005) shows that despite textural variables such as the 1.6 μm entropy provide a good separation of clouds from glint and clear ocean, textural variables others than the simple local standard variation cannot be easily applied to the whole set of ATSR-2 observations because processing to navigate forward viewing scenes into the nadir viewing observation geometry somehow perturbs the original spatial distribution of the signal.

Merchant et al. (2005) recognize the information content of complex textural variables however they select the local standard deviation over a 3x3 pixel box since its associated uncertainty may readily be related to the physical noise characteristics of the sensor, and, with $m = 9$, is a relatively precise estimator while retaining a fairly high resolution.

3.3 Angular variables

BT11n-BT11f vs BT11n-BT12n: Zavody et al (2000) introduce a cloud detection test that compares the difference between measured BT11 in the two different geometry for a given pixel, against a value predicted function of the difference **BT11n-BT12n** both measured at nadir. A similar angular test is defined combining **BT11** and **BT3.7.** The physical basis behind this kind of tests is the different atmospheric path that enhance the difference in absorption properties of water vapor and clouds. In principle, for surface with emissivity close to one, such as the ocean, no angular dependency is expected from the surface emission contribution. Over sea-ice, infrared emissivity can be lower than sea water one (Hori et al. 2006) therefore an angular dependence of the surface emission contribution is expected, however for most of the range of SLSTR viewing geometries the sensitivity should be low.

3.4 Ancillary data and parameters

Ancillary data are required to select the appropriate tests and/or the appropriate thresholds or similarly to select the relevant PDF's. In the reviewed literature the following variables have been found:

- Surface type including snow/ice mask: from this point of view this study focuses on ocean pixels, according to the adopted sea/land mask and the sea-ice coverage is expected to be a product. However, the information of depth of the ocean can be useful to discriminate between open ocean and coastal areas where, in addition to the possibility to have land contaminated pixels, the occurrence of tides may cause misclassification of pixels.
- Observation/solar illumination geometry.
- Geographical position.
- Digital Elevation Model (DEM): digital elevation model is used, for example, by cloud detection algorithm based on stereoscopic observation (e.g. Cawkwell et al. 2001). Also topography may be used, with other information such as time of the year to allow the pixel to be snow covered or not. For the purpose of this study, focusing on the ocean, there will be no need of DEM.
- Season.
- SST (climatology, forecast).
- Total Precipitable Water Vapor: in addition to the occurrence of clouds and associated radiative effects, water vapor absorption/emission is the atmospheric radiative processes that is responsible for variability in the observed radiation. Other gases absorbing/emitting within the range covered by the SLSTR channels have either a small radiative effect or are characterized by low variability.
- Surface atmospheric pressure. This variable is required in case a detailed estimation of the molecular scattering contribution is required.
- Sea surface wind: sea surface wind is needed to estimate the expected reflectance for clear sky ocean surface as well as to estimate the sun-glint area (e.g. Cox & Munk, 1954a-b).
- Aerosol optical thickness is required by some cloud detection scheme to avoid the interpretation of aerosols as optically thin clouds.
- Near surface atmospheric Temperature: A near surface, atmospheric temperature is needed to set nighttime BT11 thresholds to detect multi-layered clouds during nighttime conditions for the VIIRS cloud detection algorithm (Godin 2014).

4. Validation

A fundamental aspect, in developing a cloud detection scheme, is its validation (e.g. Ackerman et al. 2008, Rossow & Garder 1993). This is generally done by comparing the cloud detection results against an independent estimation. In literature, several sources of independent cloud detection estimation can be found.

A frequent approach is the comparison of results from an automatic cloud detection schemes against the results, over the same data set, obtained from an operator assisted classification (e.g. Bulgin et al. 2015). Operator assisted classification is considered a reliable cloud detection method because experienced operators apply, when manually classifying the images, a combination of concepts that are difficult to implement correctly in an automatic classification algorithm. However, there is a margin of subjectivity that makes such classification operator-dependent. Merchant et al. (2005) evaluated the uncertainty introduced by the different operators by comparing results of operator assisted classification performed, over the same dataset, by two different operators: they report an agreement of 98.7%.

An alternative to the comparison against operator assisted classification is the comparison against cloud cover from other satellite (e.g. Griggs & Bamber 2008) or from different algorithm applied to the same dataset (e.g. Ebert 1987).

In principle, the accuracy of statistical methods can be estimated from different runs of the method using different subset of a training dataset (e.g. Welch et al. 1992, Eberth et al. 1992).

Over Polar oceans, where there is also the issue of three classes classification (clear, sea-ice, cloudy) passive MW estimation of sea ice occurrence can be used to test the skill on se-ice detection (e.g. Ananasso et al. 2003)

Surface meteorological cloud cover observations (SYNOP) can be used as validation data source (e.g. Ebert 1989, Breon & Colzy 1999, Liberti & El Mezdari 2000, Griggs & Bamber 2008, Kotarba 2009). The standard operator estimation of cloud cover is however mostly limited to daytime and over land and refer to an area that depends from the cloud bottom height (Malberg 1973).

By assuming a space-time correspondence, time series of cloud properties profiles as obtained from surface based Lidar and Cloud Radar (e.g. Clothiaux et al. 2000) can be used to estimate the cloud cover over the measurement site in the satellite observation geometry (e.g. Ackerman et al. 2008, Liu et al. 2004, Reidi et al. 2001).

Cloud cover information can be also obtained from surface radiation measurements as LW of SW downwelling fluxes as well as from all sky cameras (e.g. Long & Ackerman 2000, Nardino et al. 2002, Werkmeister et al 1015)

From the analysis of atmospheric profiles from radiosonde data (e.g. Chemykh & Eskridge 1996) the presence of cloud, as well as its boundaries can be estimated and used for comparison against satellite derived products (e.g. Cawkwell et al. 2001).

Finally, an indirect way to estimate the efficiency of a proposed cloud detection scheme against a reference one is by comparing the statistics of the retrieved geophysical product for which the cloud detection is required. For example, the analysis of histograms of SST values over a set of data as obtained applying different cloud detection schemes can be used to assess improvements in the cloud detection process (e.g. Rossow & Garder 1993).

5. Conclusions

Discrimination between cloud, sea-ice and sea over Polar Regions with passive VIS-IR radiometry is in general a difficult task due to several factors:

- Lack of information from the solar channels due to total absence of solar radiation (during the polar night) or for low solar elevation angles;

- Relatively weak thermal contrast between Sea, Clouds and Sea-ice;
- Similar spectral signatures between sea-ice and ice-clouds;
- Low amount of available water vapour in polar atmospheres generating relatively high occurrence of thin and/or low clouds;
- Thermal structure of the atmosphere, with possible occurrence of thermal inversions.

Implementation in an operational processing chain can also add further constraints that limit the applicability of some cloud detection test.

On the basis of the literature review and taking into account the requirements of an operational processing chain, a set of variables has been selected as candidates for the definition of cloud/sea-ice/clear ocean PDF's. This preliminary selection includes variables that are expected to contain independent information as well as variables highly correlated. In this case, this selection phase will be used to select the variable with the best skill in terms of scene classification. Also, producing PDF's for redundant variables, when possible, can be also a strategy to reduce the impact in the estimation of geophysical variables of a problem in a particular sensor/channel (e.g. Gladkova et al. 2012)

From the point of view of texture variables, over Polar regions there is rich literature demonstrating the skill in discriminating between sea-ice and clouds (e.g. Ebert, 1987, 1989, 1992, Key 1990, Welch et al. 1990, 1992, Penaloza & Welch 1996, Coakley & Bretherton, 1982). This big effort in developing and testing complex textural indices was mostly driven by the lack of spectral information in the nighttime observations from the first generation of VIS-IR passive radiometers. Even if during nighttime the spectral information available from SLSTR is going to be the same as for the AVHRR-2 series, we expect to have a richer information content, with respect to AVHRR-2, due to the expected radiometric quality, the increased spatial resolution and the availability of multiangular information. Complex textural variables require for their estimation the analysis of the data over an area of several pixels, as a result the final spatial resolution of the cloud mask is going to be somehow degraded with respect to the original one. In addition, their estimation requires larger computing resources and introduce the issue of their estimation at the border of the swath. Following the suggestions of Merchant et al. (2005) in the preliminary set of candidate variables for the PDF's estimation we included only the local standard deviation of reflectance and brightness temperature over a 3x3 box.
In the following the list of candidate variables to be used to produce the three classes classification PDF's is reported with a sort description of the rationale for selecting it:

- **R0.8** the reflectance at 0.8 μm is expected to be low, for clear sky oceans, with relatively low contribution from molecular scattering and relatively, compared to the other SWIR window channel, large signal: these characteristics should allow to detect clouds and ice better than with channels in the visible portion of the solar spectrum. Being one of the basic channels since the first generation of VIS-IR radiometers on operational meteorological satellite a rich literature is available. Problems in the interpretation of the measurements can derive from occurrence of sunglint and from relatively large load of aerosols.
- **R1.3** the strong absorption from WV in this band allow the detection of relatively thin cirrus even over bright surfaces as snow/sea ice. In principle, an increase of radiance in this band can be associated to occurrence of high cloud with very little ambiguity particularly over sea.
- **R1.6** the information content useful for cloud detection/classification content in this channel derives from the relatively high imaginary part of the refractive index for ice. Because a channel in this band is present since the second generation of VIS-IR radiometers on

operational meteorological satellite a rich literature is available as a reference for the interpretation of the results.

- **R2.1** the reflectance at 2.1 μm have been added as candidate variable because there is no literature on the information content in term of sea ice/ocean/cloud classification and this study could be an occasion to document the additional (if any) information content of measurements in this band for sea-ice/cloud detection/classification. It is expected to have a strong correlation with the 1.6 μm and a lower level of the signal, however, the information of the 1.6 μm channel is already included in the NDSI.
- **NDVI** the Normalized Difference Vegetation Index is included in the candidate variables as test that check the 'whiteness' of clouds.
- **NDSI** the Normalized Difference Snow Index should be sensitive not only to the presence of ice but also on its microphysical characteristics.
- **STD_R1.6** The 1.6 μm local (3x3) standard deviation was selected as unique textural variable, among the reflectance channels, because the 1.6 μm channel because the higher sensitivity to absorption from ice, with respect to the visible channel, and the higher level of the signal, with respect to the 2.1 μm channel should allow a better skill in detecting cloud and ice. In addition, 1.6 μm spatial variability, in terms of local (32x32) histogram test is also used in the SLSTR standard cloud detection, and this should guarantee from one point of view a continuity in the cloud detection process and also the possibility to compare the PDF with the know how derived by applying the SLSTR cloud detection.
- **BT11** The brightness temperature in the 10-11 μm atmospheric window, over ocean, particularly at high latitudes, gives the brightness temperature close the one of the emitting surface. Can be used without ambiguity to detect optically thick and high clouds. On the other hand, over optically thin, in presence of temperature inversion, in presence of melting ponds over sea ice, the interpretation increases of uncertainty.
- **BT12** Same as for the TB11 except that there is a larger effect of absorption/emission from atmospheric water vapor. However, over polar regions atmospheric water vapor is relatively low and the larger sensitivity to absorption from ice should result in a better detection skill.
- **BT3.7** The brightness temperature in the 3-4 μm atmospheric window because of the dual nature of the measured radiance, from emission and, in presence of solar radiation, from scattering/reflection is expected to contain independent information with respect to the brightness temperature in the 10-12 μm. The question to test in the phase selecting the final variables for PDF's is whether this information is more easily interpreted when used in combination with other channels or if used by itself. For this reason, we could alternatively introduce, for daytime observation the **R3.7** variable defined as the reflectance component in the measured signal once subtracted the thermal one as estimated from the **BT11.**
- **BT11-BT12** The split window difference should allow the detection of relatively thin ice clouds. While over daytime the 1.3 μm channel reflectance is expected to have less ambiguity in the interpretation, during nighttime this channel combination, in nadir as well as in dual view mode is the main test to retrieve this sort of clouds. In addition, there is a rich literature on interpretation of this channel.
- **BT11-BT3.7** As mentioned in the review, this brightness temperature differences carries information from different physical processes (size of the condensed water particles, level of inhomogeneity of the scene) and therefore is expected to be extremely useful at least in detecting inhomogeneous scenes. A rich literature, also specific for polar region is also available for the interpretation of the information obtained from this channel combination.
- **BT12-BT3.7** As suggested by Liou et al (2004) over polar region, because of the relatively low water vapor amount and the high occurrence of ice cloud this channel combination can be more sensitive to occurrence of cloud and ice surfaces than the one using **BT11**. The skill in term of sea-ice/cloud/clear ocean classification of the two brightness temperature

differences will be compared in order to select one combination for the final set of variables used to produce the PDF's.

- **STD_TB12** The local standard deviation at 12 µm has been selected as textural variable for the thermal channels instead of the one at 11 µm because over polar regions the effects due to local variability of water vapor content at the level of the 3x3 pixel area should be largely negligible compared to the relatively higher sensitivity to ice absorption.
- **STD_TB3.7** The information in terms of detection skill of the 3.7 µm local standard deviation should be compared against the one in the **STD_TB12**. Because of the non-linear radiance-temperature dependence differences are expected between the two variables. The **STD_TB3.7** is expected to be more sensitive to inhomogeneous scene, however due to the nature of the signal at 3.7 µm using this variable implies producing different PDF's daytime/nighttime and even different daytime ones according with the solar illumination-observation geometry.

Acknowledgments

This study has been funded by the European Commission Copernicus programme and the results of the study are owned by European Commission.

Thanks to Dr. Federica Longo for having helped in the selection of a first set of relevant papers. A practical contribution to this review activity came from 6 students (Alice Certelli, Elisa Ciotoli, Yasmina Abdelsamad, Michela Policella, Marta Cardola, Giulia Di Carlo) of the 3rd year of the Liceo Scientifico Pasteur, Rome, Italy. Within the frame of their stage of 'Alternanza Scuola Lavoro', under the coordination of Prof. Mara De Meo, they helped in selecting, classifying and organizing the reviewed documents.

6. References

Ackerman, S. A., K. I. Strabala, W. P. Menzel, R. A. Frey, C. C.Moeller, and L. E. Gumley, 1998: Discriminating clear sky from clouds with MODIS. *J. Geophys. Res.*, **103**, 32 141–32 157.

Ackerman, S.A., R.A.Frey, K.I.Strabala, Y.Liu, L.E.Gumley, B.A.Baum, W.P.Menzel (2010): Discriminating clear-sky from cloud with MODIS algorithm theoretical basis document (MOD35). EOS ATBD, 121 pp.

Ackerman, S.A., R.E. Holz, R.Frey, E.W.Eloranta, B.C.Maddux & M. McGill (2008). Cloud Detection with MODIS. Part II: Validation; *J. Atmos. Ocean. Technol.* **25** 1073-1086

Ananasso, C., R.Santoleri, S.Marullo ,F.D'Ortenzio (2003). Remote sensing of cloud cover in the Arctic region from AVHRR data during the ARTIST experiment; *Int.J. Remote Sensing*, **24**, 3, 437-456

Baum, B. A., Tovinkere, V., Titlow, J., & Welch, R. M. (1997). Automated cloud/surface classification of global AVHRR/3 data using a fuzzy logic approach. *J. Appl. Meteorology*, **36**, 1519−1540.

Birks, A.R. (2007). Improvements to the AATSR IPF Relating to Land Surface Temperature Retrieval and Cloud Clearing over Land. AATSR Technical Note. Oxfordshire: Rutherford Appleton Laboratory. 12 pp.

Bréon, F.-M. & S.Colzy (1999): Cloud detection from the spaceborne POLDER instrument and validation against surface synoptic observations, *J. Appl. Meteor*., **38**, 777–785.

Bulgin, C.E., H.Sembhi, D.Ghent, J.J.Remedios, C.J.Merchant (2014). Cloud-clearing techniques over land for land-surface temperature retrieval from the Advanced Along-Track Scanning Radiometer; *Int. J. of Remote Sens.*, **35**, 10 3594–3615

Bulgin, C.E., S.Eastwood, O.Emburya, C.J.Merchant & C.Donlon; (2015) The sea surface temperature climate change initiative: Alternative image classification algorithms for sea-ice affected oceans; *Remote Sens. Environ* **162** 396–407.

Buriez, J.C., C. Vanbauce, F. Parol, P. Goloub, M. Herman, B. Bonnel, Y. Fouquart, P. Couvert & G. Seze (1997) Cloud detection and derivation of cloud properties from POLDER. *Int. J. Remote Sensing*, **18**, Issue 13, 2785-2813, DOI**:**10.1080/014311697217332

Cawkwell, F. G. L., J. L. Bamber & J-P. Muller, (2001). Determination of cloud top amount and altitude at high latitudes; *Geophys. Res. Letters*, **28**, n.9, 1675-1678.

Chemykh, I.V. & R.E. Eskridge (1996). Determination of cloud amount and level from radiosonde sounding. *J. Appl. Meteorol.*, **35**, 1362-1369

Clothiaux, E. E., Ackerman, T. P., Mace, G. G., Moran, K. P., Marchand, R.T., Miller, M. A., & Martner, B. E. (2000). Objective determination of cloud heights and radar reflectivities using a combination of active remote sensors at the ARM CART sites. *J. Appl. Meteor*., **39**, 645– 665.

CLOUDMAP, 2001. CLOUDMAP - Cirrus and Contrail cloud-top maps from satellites for Weather Forecasting and Climate Change Analysis: Final Report (1997 - 2000) 235 pp.

Coakley, J, & C.Bretherton (1982). Cloud cover from high-resolution scanner data: Detecting and allowing from partially filled fields of view, *J. of Geophys. Res.*, **87**, C7, 4917-4932.

Cox, C. & W. Munk (1954a). Measurement of the roughness of the sea surface from photographs of the Sun's glitter, *J. Opt. Soc. Am.*, **44**, 838–850, doi:10.1364/JOSA.44.000838

Cox, C. & W.Munk (1954b): Statistics of the sea surface derived from Sun glitter, *J. Mar. Res.,* **13**, 198–227, 1954b.

Di Girolamo, L., & R. Davies, (1994). A band-differenced angular signature technique for cirrus cloud detection, *IEEE Trans. Geoscience Remote Sensing*, **32**, no. 4, 890-896. doi: 10.1109/36.298017

Diner, D., E.Clothiaux & L.Di Girolamo (1999). MISR Multi-angle imaging spectro-radiometer algorithm theoretical basis. Level 1 Cloud detection, Jet Propulsion Laboratory, JPL D-13397.

Domine, F., R.Salvatori, L.Legagneux, R.Salzano, M.Fily, & R. Casacchia (2006). Correlation between the specific surface area and the short wave infrared (SWIR) reflectance of snow. *Cold Reg. Sci. Technol*., **46**, 60–68.

Eberhard, W. L. (2010). Correct equations and common approximations for calculating Rayleigh scatter in pure gases and mixtures and evaluation of differences, *Appl. Opt*., **49**(7), 1116-1130.

Ebert, E. (1987). A pattern recognition technique for distinguishing surface and cloud types in the polar regions, J. Climate Appl. Meteor., **26**, 1412-1427.

Ebert, E. (1989): Analysis of polar clouds from satellite imagery using pattern recognition and a statistical cloud analysis scheme. *J. Appl. Meteor*., **28**, 382–399.

Ebert, E. (1992): Pattern recognition analysis of polar clouds during summer and winter. *Int. J. Remote Sens.*, **13**, 97–109.

Fisher D., & J-P. Muller, (2012). Stereo derived cloud top height climatology over Greenland from 20 years of the Along Track Scanning Radiometer (ATSR) instruments. *International Archives of the Photogrammetry, Remote Sensing and Spatial Information Sciences,* Volume XXXIX-B8, 2012 XXII ISPRS Congress, 25 August – 01 September 2012, Melbourne, Australia. 109-113

Gafurov, A., & A.Bardossy (2009). Cloud removal methodology from MODIS snow cover product, Hydrol. Earth Syst. Sci., 13, 1361–1373, doi:10.5194/hess-13-1361-2009.

Gao, B.-C., Goetz, A. F. H., & Wiscombe, W. J., (1993): Cirrus cloud detection from airborne imaging spectrometer data using the 1.38 micron water vapor band. *Geophys. Res. Letters*, **20**(4), 301-304.

Gao, B.-C., W.Han, S.C.Tsay & N.F.Larsen (1998).Cloud Detection over the Arctic Region Using Airborne Imaging Spectrometer Data during the Daytime. *J. Appl. Meteor.*, **37**, 1421-1429.

Gladkova, I., M.D.Grossberg, F.Shahriar, G.Bonev & P. Romanov (2012). Quantitative Restoration for MODIS Band 6 on Aqua *IEEE Trans. Geosci. Remote Sens.*, **28**, n.6, 2409–2416.

Godin, R. (2014). Joint Polar Satellite System (JPSS) VIIRS Cloud Mask (VCM) Algorithm Theoretical Basis Document (ATBD). Joint Polar Satellite System (JPSS) Ground Project. Code 474. 474-00033.Revision E. pp. 101.

Griggs, J.A. & J.L.Bamber (2008). Assessment of Cloud Cover Characteristics in Satellite Datasets and Reanalysis; Products for Greenland. *J. Climate*, **21**, 1837- 1849. DOI: 10.1175/2007JCLI1570.1

Hale, G. M. & M.R. Querry (1973) Optical constants of water in the 200 nm to 200 um wavelength region, *Appl. Opt.*,**12**:555-563.

Haralick , R.M., K. S. Shammugam and I. Dinstein, (1973). Textural features for image classification", *IEEE Trans. Syst., Man, Cybern.*, vol. SMC-3, no. 6, 610-621.

Hasler, A. F. (1981), Stereographic observations from satellites: An important new tool for the atmospheric sciences., *Bull. Amer. Meteor. Soc.,* **62**, 194-212.

Hori, M., T. Aoki, T. Tanikawa, H. Motoyoshi, A. Hachikubo, K. Sugiura, T. J. Yasunari, H. Eide, R. Storvold, Y. Nakajima, F. Takahashi (2006). In-situ measured spectral directional emissivity of snow and ice in the 8–14 µm atmospheric window, Remote Sensing of Environment, **100**, 4, 486-502.

Huang, H.-L., W. L. Smith, J. Li, P. Antonelli, X. Wu, R.O. Knuteson, B. Huang, & B. J. Osborne (2004): Minimum Local Emissivity Variance Retrieval of Cloud Altitude and Effective Spectral Emissivity—Simulation and Initial Verification. *J. Appl. Meteor.* **43**, 795–809, doi: 10.1175/2090.1.

Hutchison, K.D., Mahoney, R., Vermote, E. F., Kopp, T. J., Jackson, J. M., Sei, A., & B. D. Iisager (2009).A Geometry-based Approach for Identifying Cloud Shadows in the VIIRS Cloud Mask Algorithm for NPOESS, *J. Atmos. Ocean. Technol.*, **26**, 1388–1397.

Hutchison, K.D., R.L.Mahoney & B.D. Iisager (2013a) Discriminating sea ice from low-level water clouds in split-window, midwavelength IR imagery, *Int. J. of Rem. Sensing*. **34**:20, 7131-7144, DOI:10.1080/01431161.2013.818259

Hutchison, K.D., B.D. Iisager & R.L. Mahoney (2013b). Enhanced snow and ice identification with the VIIRS cloud mask algorithm, *Remote Sensing Letters*, **4**:9, 929-936, DOI: 10.1080/2150704X.2013.815381

Inoue, T. (1985), On the temperature and effective emissivity determination of semitransparent cirrus clouds by bi-spectral measurements in the 10 µm window region, *J. Meteorol. Soc. of Japan*, 63, 88-99.

Key, J. (1990). Cloud Cover Analysis with Arctic Advanced Very High Resolution Radiometer Data 2. Classification with Spectral and Textural Measures. J. Geophys. Res., 95, NO. D6, 7661-7675

Key, J. & R.G.Barry (1989). Cloud cover analysis with Arctic AVHRR data. 1. Cloud detection, J. Geophys. Res., 94, D15, 18521–1853.

Key, J., Maslanik, J. A., & Schweiger, A. J. (1989). Classification of merged AVHRR/3 and SMMR Arctic data with neural networks. *Photogrammetric Engineering and Remote Sensing*, **55**, 1331−1338.

Kotarba, A.Z. (2009) A comparison of MODIS-derived cloud amount with visual surface observations, Atmospheric Research, **92**, 4, 522-530

Kou, L., D. Labrie & P. Chylek (1993), Refractive indices of water and ice in the 0.65- to 2.5 µm spectral range, *Appl. Opt.*, **32**, 3531– 3540.

Li, Z., J. Li, W.P. Menzel, T.J.Schmit & S.A. Ackerman (2007) Comparison between current and future environmental satellite imagers on cloud classification using MODIS *Remote Sensing of Environment*, **108**, 311–326

Li, J., Menzel, W. P., Yang, Z., Frey, R. A., & Ackerman, S. A. (2003). High spatial- resolution surface and cloud-type classification from MODIS multispectral band measurements. *J. Appl. Meteorology*, **42**, 204−226.

Liberti G.L., & H.El Mezdari, (2000) Comparison SPOT cloud cover quality index against meteorological surface observations. *Int. J. of Rem. Sensing*. **21**, 12, 2439-2461.

Liu, Y., J. R. Key, R. A. Frey, S. A. Ackerman & W. P. Menzel (2004). Nighttime polar cloud detection with MODIS. *Remote Sens. Environ.*, **92**, 181–194.

Long, C.N., & T. P. Ackerman. (2000). Identification of clear skies from broadband pyranometer measurements and calculation of downwelling shortwave clouds effects. *J. Geophys. Res.*, **105**, No. D12, pp.15609-15626.

Lorenz, D., 1985. On the feasibility of cloud stereoscopy and wind determination with the along-track scanning radiometer. *Int. J. Rem. Sens*., 6 (8), pp. 1445-1461.

Lubin, D., & R. A. Massom, 2006, *Polar Remote Sensing. Volume 1: Atmosphere & Polar Oceans*, Praxis/Springer. Chichester, UK, and Berlin, Germany, 756 pages.

Lyapustin, A., & Y.Wang (2009). The time series technique for aerosol retrievals over land from MODIS, in: Satellite Aerosol Remote Sensing over Land, edited by: Kokhanovsky A.A., de Leeuw, G., Springer Praxis Publ. Chichester, 69–99.

Lyapustin, A., Y.Wang & R.Frey (2008) An automated cloud mask algorithm based on time series of MODIS measurements, *J. Geophys. Res.*, **113**, D16207, doi:10.1029/2007JD009641.

Mackie, S., O. Embury, C. Old, C. J. Merchant & P. Francis (2010a); Generalized Bayesian cloud detection for satellite imagery. Part 1: Technique and validation for night-time imagery over land and sea; *Int. J. Remote Sensing*. **31**, 10, 2573-2594.

Mackie, S., O. Embury, C. Old, C. J. Merchant & P. Francis (2010b); Generalized Bayesian cloud detection for satellite imagery. Part 2: Technique and validation for day-time imagery; *Int. J. Remote Sensing*. **31**, 10, 2595-2621.

Malberg, H., (1973). Comparison of mean cloud cover obtained by satellite photographs and ground-based observations over Europe and the Atlantic. *Monthly Weather Review*, **101**, 893–897.

Martins, J.V., Tanré, D., Remer, L., Kaufman, Y., Mattoo, S., & R. Levy (2002). MODIS Cloud screening for remote sensing of aerosols over oceans using spatial variability, Geophys. Res.Lett., 29(12), 8009, doi:10.1029/2001GL013252.

Massom, R.A., & D.Lubin, (2006), *Polar Remote Sensing. Volume 2: Ice Sheets*, Praxis/Springer. Chichester, UK, and Berlin, Germany, 426 pages.

Menzel,w.P., , W. L. Smith, and T. R. Stewart, (1983): Improved cloud motion wind vector and altitude assignment using VAS. *J. Climate Appl. Meteor.,* **22,** 377–384.

Merchant, C. J., Harris, A. R., Maturi, E., & MacCallum, ,S. (2005). Probabilistic physically based cloud screening of satellite infrared imagery for operational sea surface temperature retrieval. Quarterly Journal of the Royal Meteorological Society. 131, 2735-2755.

Manuel A. Penaloza, Ronald M. Welch. (1996) Feature selection for classification of polar regions using a fuzzy expert system. *Remote Sensing of Environment* **58**, 81-100.

Muller, J.-P., Denis, M.-A., Dundas, R.D., Mitchell, K.L., Naud, C., & Mannstein, H. (2007). Stereo cloud-top heights and cloud fraction retrieval from ATSR-2. *Int. J. Remote Sensing*., **28**, n.9, 1921-1938

Nardino, M., F.Calzolari, A.Orsini & T.Georgiadis (2002). Cloud cover validation through ground-based measurements of solar radiation. *Proc. Italian Physical Soc.*, Ed. Compositori, **80**, 163-174

New, M., D. Lister, M. Hulme, & I. Making (2002). A High-Resolution Data Set of Surface Climate over Global Land Areas. *Climate Research* **21**: 1–25. doi:10.3354/cr021001.

Nolin, A. W., & Dozier, J. (1993). Estimating snow grain size using AVIRIS data. *Remote Sensing of Environment*, 44, 231−238.

Pearson, K., O. Embury, C. Bulgin, C. J. Merchant (2014). Bayesian Cloud Detection Algorithm Theoretical Basis Document; EUM-BC-ATBD-003; *Univ. of Reading,*EUMETSAT Bayesian Cloud Detection, Final Issue 1, 1-56

Poulsen, C.A., R. Siddans, G.E.Thomas, A.M.Sayer, R. G. Grainger, E. Campmany, S.M.Dean, C.Arnold & P.D. Watts (2012). Cloud retrievals from satellite data using optimal estimation: evaluation and application to ATSR. *Atmos. Meas. Tech.*, **5**, 1889–1910. doi:10.5194/amt-5-1889-2012

Prata, A & P. Turner. (1997). Cloud-top determination using ATSR data. *Remote Sensing Environ.*, 59(1), 1-13.

Riedi,J., P.Goloub & R.T. Marchand (2001) Comparison of POLDER cloud phase retrievals to active remote sensors measurements at the ARM SGP site. *Geophys. Res. Letters*, **28**, 11, 2185-2188.

Rossow W.B., & L.C. Garder, (1993). Validation of ISCCP Cloud Detections. *J. Climate,* **6**, 2370–2393.

Salomonson,V.V. & I. Appel (2004). Estimating fractional snow cover from MODIS using the normalized difference snow index. *Remote Sensing of Environment*, **89**, 351 – 360.

Saunders, R.W. & Kriebel, K.T. (1988) An improved method for detecting clear sky and cloudy radiances from AVHRR data. Int. J. Remote Sensing, 9, 123–150.

Sayer,A.M., G. E. Thomas & R. G. Grainger (2010). A sea surface reflectance model for (A)ATSR, and application to aerosol retrievals. *Atmos. Meas. Tech.*, **3**, 813–838. doi:10.5194/amt-3-813-2010

Simpson, J.J. & R.H. Keller (1995). An Improved Fuzzy Logic Segmentation of Sea Ice, Clouds, and Ocean in Remotely Sensed Arctic Imagery0; *Remote Sensing of Environment*, **54**, 290- 312.

Simpson, J.J., Y.L.Tsou, A.Schmidt, A.Harris (2005). Analysis of Along Track Scanning Radiometer-2 (ATSR-2) data for clouds, glint and sea surface temperature using neural networks, Remote Sensing of Environment, 98, 2–3, 152-181, ISSN 0034-4257

Stamnes, K., Li, W., Eide, H., Aoki, Te., Hori, M., & Storvold, R. (2007). ADEOS-II/GLI snow/ice products — Part I: Scientific basis. *Remote Sensing Environment*. 111, 2-3, 258-273. doi:10.1016/j.rse.2007.03.023

Tedesco, M. & A.A. Kokhanovsky (2007). The semi-analytical snow retrieval algorithm and its application to MODIS data, *Remote Sens. Environ*., **110**, 317–331.

Temimi, M., P. Romanov, H. Ghedira, R. Khanbilvardi & K. Smith (2011): Sea-ice monitoring over the Caspian Sea using geostationary satellite data, *International Journal of Remote Sensing*, **32**:6, 1575-1593

Tucker, C.J., (1979). Red and photographic infrared linear combinations for monitoring vegetation, *Remote Sensing of Environment*, **8**, 127-150.

Vasilkov,A., J.Joiner, R.Spurr, P.K. Bhartia, P.Levelt, & G.Stephens (2008). Evaluation of the OMI cloud pressures derived from rotational Raman scattering by comparisons with other satellite data and radiative transfer simulations *J. Geophys. Res*, **113**, D15S19, doi:10.1029/2007JD008689.

Warren, S.G. & R.E. Brandt (2008). Optical constants of ice from the ultraviolet to the microwave: A revised compilation. *J Geophys Res.* ;**113**:D14220,10 pp. doi:10.1029/2007JD009744.

Warren, S. G.,& W.J.Wiscombe (1980). A model for the spectral albedo of snow. II: Snow containing atmospheric aerosols, *J. Atmos. Sci.* **37**, 2734–2733.

Welch R.M., S.K.Senguptaa, A. K. Gorocha, P.Rabindrab, N.Rangarajb & M.S.Navar (1992) Polar Cloud and Surface Classification Using AVHRR Imagery: An Intercomparison of Methods, *J. Appl. Meteor.*, **31**, 5, 406-419.

Welch, R. M., Kuo, K. S., & Sengupta, S. K. (1990). Cloud and surface textural features in polar regions. *IEEE Trans. Geosci. Remote Sens*., **28**, 520–528.

Werkmeister, A., Lockhoff, M., Schrempf, M., Tohsing, K., Liley, B., & Seckmeyer, G. (2015): Comparing satellite- to ground-based automated and manual cloud coverage observations – a case study, *Atmos. Meas. Tech*., 8, 2001-2015, doi:10.5194/amt-8-2001-2015.

Wind,G., S.Platnick, M.D. King, P.A. Hubanks, M.J. Pavolonis, A.K. Heidinger, P.Yang & B.A. Baum (2010). Multilayer Cloud Detection with the MODIS Near-Infrared Water Vapor Absorption Band. *J. Appl. Meteor. Climatol*., **49**, 2315–2333. DOI: 10.1175/2010JAMC2364.1

Yamanouchi, T., Suzuki, K., & Kawaguchi, S. (1987). Detection of clouds in Antarctica from infrared multispectral data of AVHRR. *J. Meteor. Soc. of Japan*, **65**, 949–962.

Zavody, A.M., P.D.Watts, D. L. Smith, & C. T. Mutlow (1998). A Novel Method for Calibrating the ATSR 2 1.6 µm Channel Using Simultaneous Measurements Made in the 3.7µm Channel in Sun Glint. *J. Atmos. Ocean. Technol.* **15** 1243-1252.

Zavody, A.M., C. T.Mutlow & D.T. Llewellyn-Jones (2000). Cloud Clearing over the Ocean in the Processing of Data from the Along-Track Scanning Radiometer (ATSR). *J. Atmos. Ocean. Technol.* **17** 595-615.

Appendix 1: Channel characteristics for the reviewed sensors

SLSTR

Channel	λ centre (μm)	Width (μm)
S1	0.555	0.02
S2	0.659	0.02
S3	0.865	0.02
S4	1.375	0.015
S5	1.61	0.06
S6	2.25	0.05
S7	3.74	0.38
S8	10.85	0.9
S9	12	1
F1	3.74	0.38
F2	10.85	0.9

(A)ATSR, ATSR-2, ATSR

Channel	λ centre (μm)	Width (μm)
1 (S1)	*0.550*	*0.02*
2 (S2)	*0.659*	*0.02*
3 (S3)	*0.865*	*0.02*
4 (S5)	1.61	0.3
5 (S7)	3.70	0.3
6 (S8)	10.85	1.0
7 (S9)	12	1

AVHRR

Channel	Bandwidth (μm)
1 (S2)	0.58 - 0.68
2 (S3)	0.725 - 1.00
3A (S5)	1.58 - 1.64
3B (S7)	3.55 - 3.93
4 (S8)	10.30 - 11.30
5 (S9)	11.50 - 12.50

MODIS

Channel	Bandwidth (μm)
1(S2)	0.620–0.670
2	0.841–0.876
3	0.459 – 0.479
4(S1)	0.545 – 0.565
5	1.230 – 1.250
6 S5	1.628 – 1.652
7 S6	2.105 – 2.155
8	0.405 – 0.420
9	0.438 – 0.448
10	0.483 – 0.493
11	0.526 – 0.536
12	0.546 – 0.556
13	0.662 – 0.672
14	0.673 – 0.683
15	0.743 – 0.753
16(S3)	0.862 – 0.877
17	0.890 – 0.920
18	0.931 – 0.941
19	0.915 – 0.965
20 S7	3.660 - 3.840
21	3.929 - 3.989
22	3.929 - 3.989
23	4.020 - 4.080
24	4.433 - 4.498
25	4.482 - 4.549
26 S4	1.360 - 1.390
27	6.535 - 6.895
28	7.175 - 7.475
29	8.400 - 8.700
30	9.580 - 9.880
31 S8	10.780 - 11.280
32 S9	11.770 - 12.270
33	13.185 - 13.485
34	13.485 - 13.785
35	13.785 - 14.085
36	14.085 - 14.385

GLI

Channel	Central Wavelength (μm)	Width (μm)

1	0.380	0.01
2	0.400	0.01
3	0.412	0.01
4	0.443	0.01
5	0.460	0.01
6	0.490	0.01
7	0.520	0.01
8 **S1**	0.545	0.01
9 **S1**	0.565	0.01
10	0.625	0.01
11 **S2**	0.666	0.01
12	0.680	0.01
13	0.678	0.01
14	0.710	0.01
15	0.710	0.01
16	0.749	0.01
17	0.763	0.01
18 **S3**	0.865	0.01
19	0.865	0.01
20	0.460	0.07
21	0.545	0.05
22	0.660	0.06
23	0.825	0.11
24	1.050	0.02
25	1.135	0.07
26	1.240	0.02
27 S4	1.380	0.04
28 S5	1.640	0.20
29 **S6**	2.210	0.22
30 S7	3.715	0.33
31	6.7	0.50
32	7.3	0.50
33	7.5	0.50
34	8.6	0.50
35 **S8**	10.8	1.00
36 **S9**	12.0	1.00

	Wavelength (µm)	(µm)
M1	0.412	0.02
M2	0.445	0.018
M3	0.488	0.02
M4 **S1**	0.555	0.02
M5(B) **S2**	0.672	0.02
M6	0.746	0.015
M7(G) **S3**	0.865	0.039
M8	1.240	0.02
M9 **S4**	1.378	0.015
M10 S5	1.610	0.06
M11 **S6**	2.25	0.05
M12 S7	3.700	0.18
M13	4.05	0.155
M14	8.55	0.30
M15 **S8**	10.763	1.00
M16 **S9**	12.013	0.95
DNB	0.7	0.4
I1(B)	0.64	0.08
I2(G)	0.865	0.039
I3(R)	1.61	0.06
I4 S7	3.74	0.38
I5	11.45	1.9

VIIRS

Channel	Central	Width